PHYSICAL REVIEW A **92**, 041804(R) (2015)

Fractional averaging of repetitive waveforms induced by self-imaging effects

Luis Romero Cortés,* Reza Maram, and José Azaña
Institut National de la Recherche Scientifique–Énergie, Matériaux et Télécommunications (INRS-EMT), 800 de la Gauchetière Ouest, Suite 6900, H5A 1K6 Montréal, Québec, Canada
(Received 1 June 2015; published 12 October 2015)

We report the theoretical prediction and experimental observation of averaging of stochastic events with an equivalent result of calculating the arithmetic mean (or sum) of a *rational* number of realizations of the process under test, not necessarily limited to an integer record of realizations, as discrete statistical theory dictates. This concept is enabled by a passive amplification process, induced by self-imaging (Talbot) effects. In the specific implementation reported here, a combined spectral-temporal Talbot operation is shown to achieve undistorted, lossless repetition-rate division of a periodic train of noisy waveforms by a rational factor, leading to local amplification, and the associated averaging process, by the fractional rate-division factor.

DOI: 10.1103/PhysRevA.92.041804 PACS number(s): 42.30.Kq, 06.60.Jn, 42.30.Lr, 42.30.Va

The Talbot effect, or self-imaging, was first observed and explained in the problem of diffraction of spatially periodic wave fields [1,2], and later extended and extensively applied across many different regimes [3], including matter waves [4], quantum wave functions [5], x-ray diffraction [6], crystal nonlinearity [7], laser physics [8], etc. Manifestations of the Talbot effect have been also described in the temporal domain [9], spectral domain [10], and angular spectrum domain [11]. This Rapid Communication describes a conceptual feature of the Talbot effect, namely, its capability to achieve statistical averaging of an ensemble of realizations of a given stochastic process, where the number of averaged realizations can be any given *fractional* number. Strikingly, such a capability enables statistical calculations that are "forbidden" by the mathematical definition of discrete averaging, which is strictly limited to application on an integer number of realizations of the process under test.

The mathematical operation of averaging is a fundamental one in the context of stochastic processes, simply involving calculation of the arithmetic mean (essentially, a sum) of multiple realizations of the process under analysis [12]. Besides its intrinsic mathematical interest, statistical averaging has found many important applications: it has proved to be particularly useful as a very direct way of reducing undesired random noiselike fluctuations in classical [13] and quantum-probability waveforms [14–17] in any of the different available measurement domains, e.g., for spatial-domain, time-domain, or frequency-domain wave fields. Obviously, the arithmetic mean must be calculated over a discrete set of realizations of the signal of interest, which necessarily implies that intrinsically, only *integer averaging* is mathematically allowed.

The work reported in [18] showed how a combination of spectral and temporal Talbot effects can be used to divide the repetition rate of a periodic waveform train by any integer factor, N, using energy-preserving mechanisms, thus producing undistorted passive amplification of each resulting individual waveform. Such a process can be interpreted as the result of coherent addition of every N input waveform, so that it produces a noise-reduction outcome, equivalent to that of statistical averaging of N waveforms.

In this work, we show further that the Talbot amplification concept is not limited to integer gain factors but rather, it can be extended to realize repetition rate division and the associated passive amplification process of the original waveform train by any desired fractional factor (i.e., a rational number). This suggests the possibility of achieving *fractional averaging* of the original repeating waveforms. We provide experimental results on the effective averaging operation that is inherently implemented by the process, and conclude that the resulting statistics are fully consistent with an equivalent average of a rational number of recorded measurements. Notice that the specific time-domain implementation reported and studied here provides a very convenient platform for experimental analysis of the introduced fractional averaging concept. However, we recall that the concept is not restricted to application on periodic time-domain waveforms, yet at any wavelength regime, but can be also extended for application across any of the manifestations of the Talbot effect, including periodic one-dimensional (1D) and two-dimensional (2D) spatial objects, frequency combs, quantum wave functions, matter waves, etc.

Figure 1(a) shows the temporal Talbot carpet, representing the evolution of the instantaneous power of a periodic train of optical pulses along its propagation through a second-order dispersive medium (i.e., one providing a linear group delay variation through the entire pulse bandwidth). Dispersive propagation speeds up and slows down the different frequency components of the train, originally in-phase, redistributing its energy into different temporal intensity patterns. The Talbot condition, given in Eq. (1) below, allows one to calculate the total group-velocity dispersion (GVD) associated with each Talbot (sub-)image [9].

$$2\pi|\ddot{\phi}| = \frac{s}{m}t_r^2, \tag{1}$$

where $\ddot{\phi} = \beta_2 z$ is the slope of the group delay versus radial frequency of the dispersive medium, β_2 is the second-order dispersion coefficient (GVD per unit length, around the pulses' central angular frequency), z is the propagation length in the medium, $t_r = 1/\nu_r$ is the temporal period of the original pulse train (i.e., the inverse of the repetition rate), ν_r [which

*romero@emt.inrs.ca

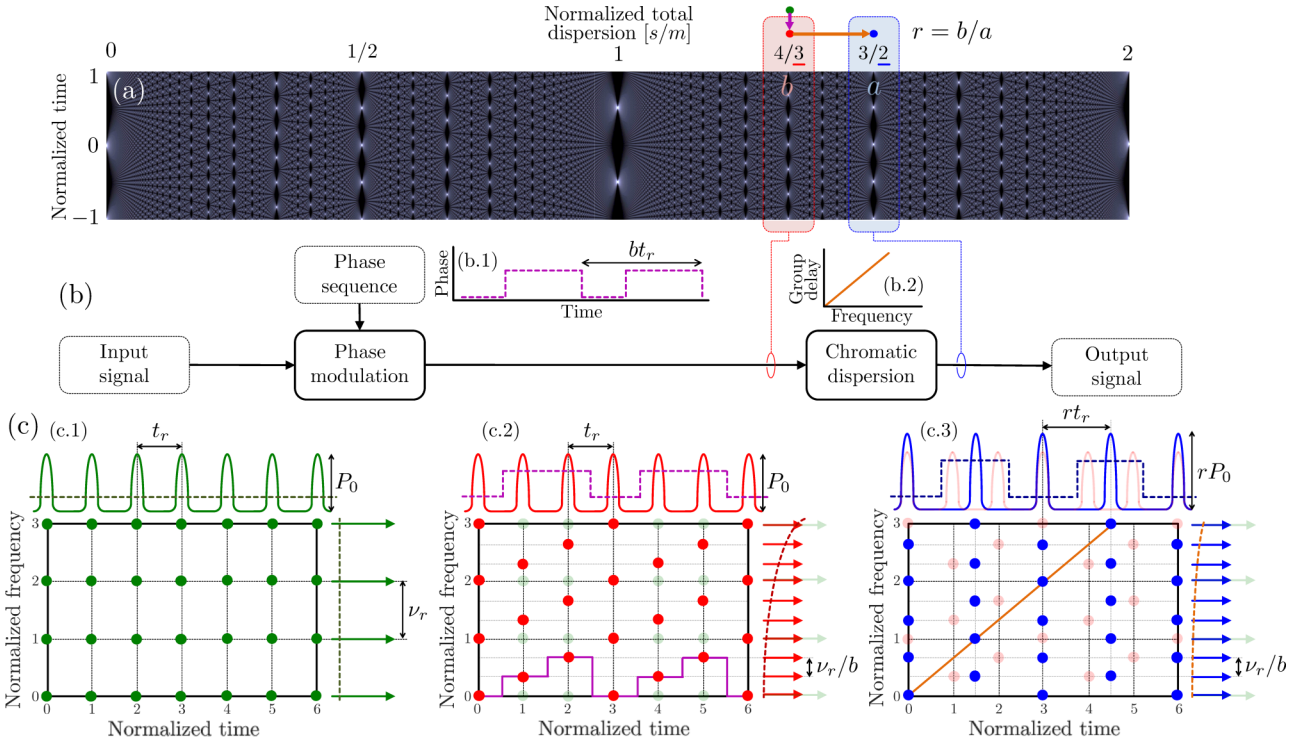

FIG. 1. (Color online) Operation principle and example case $r = b/a = 3/2$. (a) Temporal Talbot carpet. (b) Block diagram: (b.1) prescribed phase sequence; (b.2) prescribed group delay versus frequency profile. (c) Time-frequency representation of the involved signals: (c.1) input train; (c.2) phase-conditioned train; (c.3) rate-divided train.

dictates the free spectral range (FSR) of the corresponding frequency comb representation of the train], and s and m are two mutually prime natural numbers. Talbot images, where the input pulse period is preserved, are formed at integer values of s/m (i.e., $m = 1$), while Talbot subimages, where the input pulse period is divided by the integer factor m, are formed at rational values of s/m (i.e., $m > 1$). An interesting feature of the effect is that each Talbot subimage has an associated deterministic phase profile, consisting of a discrete sequence of pulse-to-pulse phase steps that follow a quadratic law [19,20]. Introducing these phase profiles to the input train, either by electro-optic means [21] or by the assistance of a nonlinear process [22], will emulate previous dispersive propagation of a hypothetical flat-phase pulse train, first launched at the input of the dispersive medium ($z = 0$), with repetition rate divided by the factor m. Notice that the mentioned temporal phase modulation induces a spectral self-imaging effect on the original optical pulse train [23], so that the FSR of the associated periodic frequency comb is divided by the factor m, consistently with the mentioned rate division for the hypothetical input pulse train at $z = 0$. The resulting pulse train after phase modulation can then be used as a starting point inside the Talbot carpet to achieve repetition rate division by further dispersive propagation to a different (lower rate) Talbot subimage.

Generally, the rate-division factor can be designed to be any desired rational number, expressed as $r = b/a$, where b and a are two mutually prime natural numbers and $a < b$, i.e., $r \in \mathbb{Q}$ and $r > 1$. Figure. 1(b) illustrates the conceptual block diagram of the process. Figure 1(c) shows a joint time-frequency representation of the involved signals. The example shown in Fig. 1 illustrates the scenario of repetition rate division by the factor $r = 3/2$, i.e., two pulses are generated at the output of the system in the time span corresponding to three consecutive input pulses. First, the input train [Fig. 1(c.1)] is phase modulated to achieve spectral self-imaging by the factor $b = 3$, producing an FSR of $\nu_r/3$ [Fig. 1(c.2)]. This is equivalent to a predispersed input pulse train with a period of $3t_r$ to obtain an $m = 3$ Talbot subimage. Second, this phase-modulated signal is further dispersed to reach a Talbot subimage of the equivalent rate-divided train by $a = 2$ [Fig. 1(c.3)]. The output period is then given by $rt_r = 3/2t_r$, having achieved the target fractional rate-division process.

The temporal phase to be applied to the nth pulse of the sequence, $\varphi[n]$, and the total dispersion required to achieve repetition rate division by the factor r can be derived from the well-known spectral and temporal Talbot conditions [9,23], and are given by Eq. (2) and Eq. (3), respectively.

$$\frac{\varphi[n]}{\pi} = \pm \mathrm{sgn}\{\beta_2\} \frac{b \mp 1}{b} n^2, \tag{2}$$

$$2\pi |\beta_2| z = (bt_r)^2 \left| p + \frac{q}{a} - \frac{1}{b} \right|, \tag{3}$$

where $\mathrm{sgn}\{\cdot\}$ is the sign operator, p and q are two positive integers, and $q > 0$ is mutually prime with a. The case $\{p = 0, q = 1\}$ minimizes the required GVD for a given input repetition rate. The sequence defined in Eq. (2) is b periodic if reduced modulo π or 2π.

The described process involves phase-only operations exclusively (i.e., temporal phase modulation and spectral

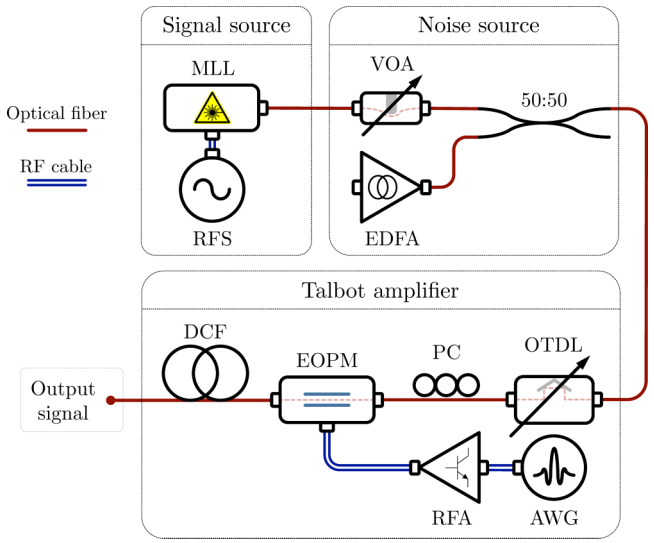

FIG. 2. (Color online) Experimental setup. MLL: mode-locked laser, RFS: radio-frequency synthesizer, VOA: variable optical attenuator, EDFA: erbium-doped fiber amplifier, OTDL: optical tunable delay line, PC: polarization controller, AWG: arbitrary waveform generator, RFA: radio-frequency amplifier, EOPM: electro-optic phase modulator, DCF: dispersion-compensating fiber.

phase filtering), which are inherently energy-preserving mechanisms. As such, conservation of energy states that the energy of each individual output pulse will be increased with respect to the input by the rate-division factor, r (except for the involved practical passive losses). This is the fundamental principle of the Talbot amplification concept, here generalized to fractional gain factors. Previously, it was shown how an integer Talbot amplifier with an amplification factor of $N \in \mathbb{N}$ generates an output waveform which in terms of noise, is equivalent to a classical averaging process of N realizations of the input waveform [18]. The generalized Talbot amplifier described by Eqs. (2) and (3) will implement the fractional amplification factor $r \in \mathbb{Q}$. As such, we predict that this system will produce an equivalent *fractional averaging* process, such as if the mean had been calculated over a "rational number" of recorded waveforms. In sharp contrast to a conventional averaging operation, the concept of fractional averaging is possible in the context of self-imaging since there is no one-to-one relationship between input and output pulses in a Talbot amplifier; instead, each output pulse is built from contributions (interference) of many consecutive input pulses, and the same input pulse contributes to the formation of several different output pulses. In what follows, we report experimental validation of the concept of fractional Talbot amplification and the related averaging process.

Figure 2 shows a schematic of the used experimental setup. An actively mode-locked laser is driven by a radio-frequency synthesizer, tuned at the desired input repetition rate. This setup delivers a flat-phase train of 6 ps full width at half maximum (FWHM) Gaussian-like transform-limited optical pulses, at a central wavelength of 1550 nm. The corresponding spectrum is a coherent optical frequency comb. This signal is then injected with amplified spontaneous emission (ASE) from an open-input erbium-doped fiber amplifier, connected via a 3 dB directional fiber coupler. This system can be modeled as a source of additive white Gaussian noise (AWGN), as long as the complete signal bandwidth is covered by the amplification bandwidth [24]. A variable optical attenuator is used to maintain a specific level of input optical signal-to-noise ratio (OSNR). The prescribed temporal phase modulation profile, calculated from Eq. (2), is generated by a 24 Gsps electronic arbitrary waveform generator and introduced to the signal by a 40 GHz electro-optic phase modulator. The phase-conditioned signal is finally propagated through a dispersion-compensating fiber with total GVD satisfying Eq. (3).

TABLE I. Experimental results.

	Input		Output		Configuration	
	$\nu_r^{(i)}$[a]	$t_r^{(i)}$[b]	$\nu_r^{(o)}$[c]	$t_r^{(o)}$[d]	$b/a = r$[e]	$D \cdot z$[f]
(1)	7.928	126.139	5.946	168.185	$4/3 \simeq 1.333$	−2649.071
(2)	11.892	84.092	7.928	126.139	$3/2 = 1.5$	−1324.535
(3)	12.535	79.777	7.521	132.962	$5/3 \simeq 1.667$	−2649.071
(4)	15.731	63.568	8.989	111.244	$7/4 = 1.75$	−2649.071
(5)	18.802	53.185	7.521	132.962	$5/2 = 2.5$	−2649.071
(6)	15.856	63.069	5.946	168.185	$8/3 \simeq 2.667$	−6622.677
(7)	15.898	62.902	4.542	220.157	$7/2 = 3.5$	−8646.204

[a]Configured input repetition rate (GHz).
[b]Configured input pulse period (ps).
[c]Measured output repetition rate (GHz).
[d]Measured output pulse period (ps).
[e]Implemented rate-division factor. All the cases satisfy Eq. (3) for the condition of minimum dispersion $\{p = 0, q = 1\}$.
[f]Total second-order chromatic dispersion (ps/nm).

Table I presents the set of tested experimental conditions and obtained fractional rate-division results. The dispersion coefficient D (second-order dispersion per unit length, around the central wavelength, λ), given in ps/nm/km in Table I, follows the conversion law $D = -2\pi\beta_2 c/\lambda^2$, where c is the speed of light in the vacuum.

Figure 3 (a) shows the phase modulator drive voltages, as prescribed by Eq. (2), for the configurations listed in Table I. The anticipated spectral self-imaging effect is observed in the measured optical spectra, in Fig. 3(b), leading to the expected FSR division by the factor b. Figure 4 (a) shows the temporal traces of the input and output trains, in the absence of noise, as recorded by a 500 GHz bandwidth optical sampling oscilloscope. The amplitudes are normalized to the peak power of the input signal. To establish a fair definition of the gain in the system, the total passive input-to-output loss of the setup (13.5 dB) is accounted for, and thus we compare with a correspondingly attenuated version of the input train. In this situation the system presents a power gain of r. Figure 4(b) shows the measured input and output radio-frequency spectra, verifying the correct fractional rate division. It is also important to mention that as expected for a self-imaging effect, the individual output pulses are nearly undistorted copies of the input ones.

The central and perhaps most interesting result of this work is on the predicted fractional averaging effect. In order to quantify the effect of averaging of the noise in the output pulses, we calculate the coefficient of variation, CV, of the ASE

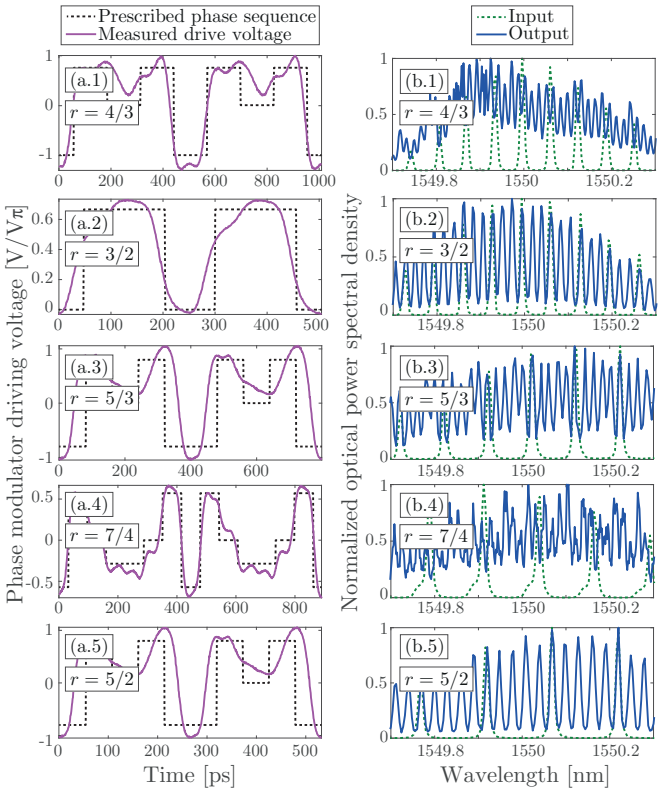

FIG. 3. (Color online) Experimental results. (a) EOPM drive voltages (solid line) and prescribed phase sequences (dashed line). (b) Optical power spectra of the input (dashed line) and output (solid line) signals.

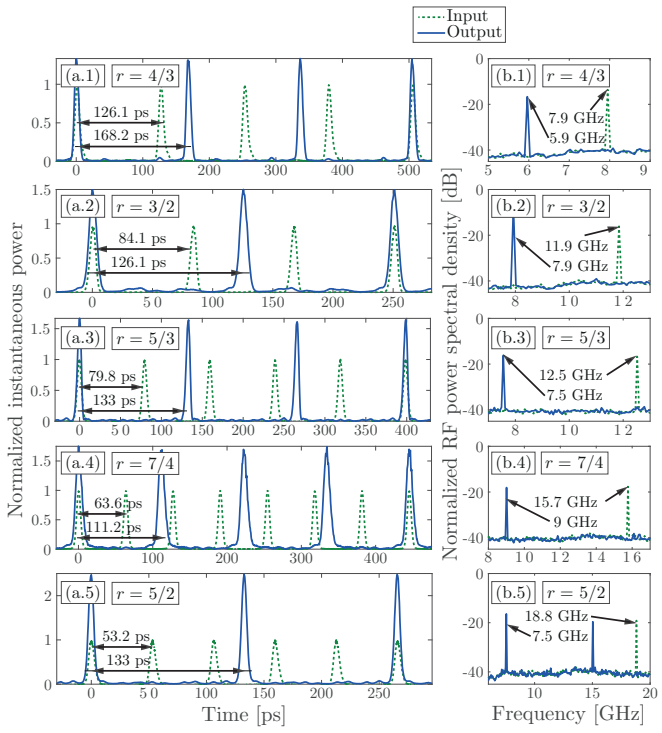

FIG. 4. (Color online) Experimental results. (a) Temporal traces of the input (dashed line) and output (solid line) signals. (b) Radio-frequency spectra of the input (dashed line) and output (solid line) signals.

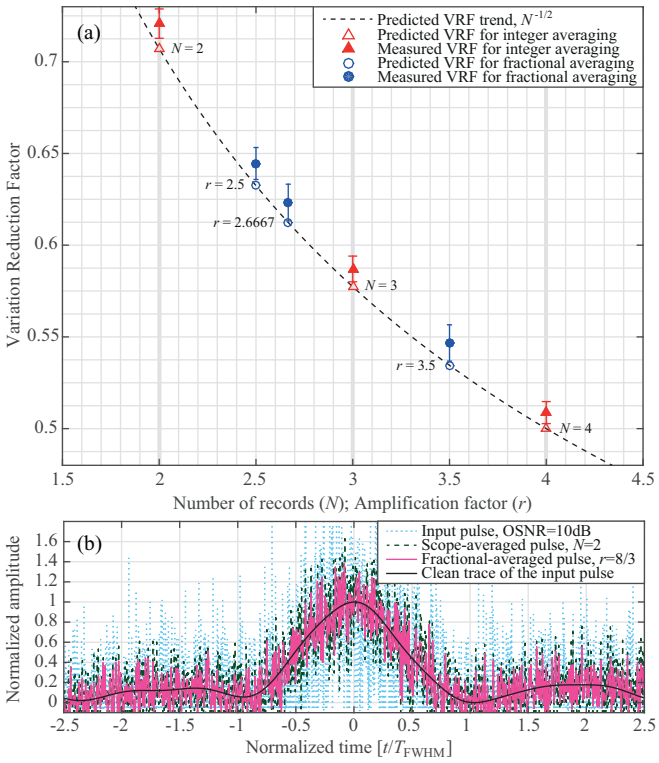

FIG. 5. (Color online) Noise analysis of the experimental results. (a) VRF versus rate-division factor r, and record length N. (b) Single-shot traces of the input and output pulses for fractional averaging ($r = 8/3 \simeq 2.667$) and $N = 2$ times scope averaging. The time scale is normalized to the FWHM of the input pulse, and the power scale is normalized to the input peak power.

fluctuations around the peak intensity level of the measured pulses (defined as the ratio of the standard deviation to the mean of the fluctuations) [25]. In particular, the used figure of merit is the ratio of the coefficient of variation of the individual output pulses (e.g., for an averaging process of $N \in \mathbb{N}$ measurements), CV_N, to that of the individual input pulses, CV_1. We label this figure of merit as the "variation reduction factor," $\mathrm{VRF} = \mathrm{CV}_N/\mathrm{CV}_1$. As predicted by the classical central limit theorem [12], if the measured samples are independent and identically distributed (as is the case for AWGN processes), this ratio scales as $N^{-1/2}$. In [18] it was shown how an integer Talbot amplifier verifies this VRF trend with N playing the role of the power gain, or equivalently, the rate-division factor. It is only reasonable to assume that the same principle will apply to a fractional rate-division process with $N \leftarrow r$, i.e., a situation equivalent to the averaging of $r \in \mathbb{Q}$ samples.

Figure 5 (a) shows the measured VRF after the fractional averaging process, in comparison with the result obtained by (integer) averaging in a sampling oscilloscope, with equal OSNR (set to 10 dB). The obtained VRF for the evaluated fractional repetition rate division (and associated fractional passive amplification) cases precisely follows the expected trend $r^{-1/2}$. This result corresponds to interpolations in between the values obtained by conventional scope averaging (where the VRF is originally defined), generally following the theoretical trend $N^{-1/2}$. Hence, as predicted, the Talbot amplification process

implements an averaging operation where the record length is effectively equal to the rational number r.

For completeness, Fig. 5(b) shows an example of measured temporal traces for a rate-division factor of $r = 8/3 \simeq 2.6667$, together with an $N = 2$ times averaged pulse, captured by an electrical sampling oscilloscope equipped with a 45 GHz bandwidth photodiode.

In summary, this work reports the theoretical prediction and experimental observation of a process of statistical averaging with an effective result of calculating the arithmetic mean of a rational number of measurements, a strikingly counterintuitive operation enabled by self-imaging passive amplification. In the specific reported implementation, we employ a specific realization of combined spectral-temporal Talbot effects to induce undistorted, lossless repetition-rate division of a periodic train of optical waveforms by a rational factor, leading to the corresponding fractional amplification and averaging of the individual input waveforms. This unique concept represents a generalization of the conventional operation of discrete statistical averaging, enabling an unprecedented, wider range of mathematical and experimental conditions.

[1] H. F. Talbot, Philos. Mag. **9**, 401 (1836).
[2] Lord Rayleigh, Philos. Mag. **11**, 196 (1881).
[3] J. Wen, Y. Zhang, and M. Xiao, Adv. Opt. Photonics **5**, 83 (2013).
[4] J. Ruostekoski, B. Kneer, W. P. Schleich, and G. Rempe, Phys. Rev. A **63**, 043613 (2001).
[5] X.-B. Song, H.-B. Wang, J. Xiong, K. Wang, X. Zhang, K.-H. Luo, and L.-A. Wu, Phys. Rev. Lett. **107**, 033902 (2011).
[6] F. Pfeiffer, T. Weitkamp, O. Bunk, and C. David, Nat. Phys. **2**, 258 (2006).
[7] Y. Zhang, J.-M. Wen, S. N. Zhu, and M. Xiao, Phys. Rev. Lett. **104**, 183901 (2010).
[8] H. Guillet de Chatellus, E. Lacot, W. Glastre, O. Jacquin, and O. Hugon, Phys. Rev. A **88**, 033828 (2013).
[9] J. Azaña and M. A. Muriel, IEEE J. Sel. Top. Quant. Electron. **7**, 728 (2001).
[10] J. Azaña, Opt. Lett. **30**, 227 (2005).
[11] J. Azaña and H. Guillet de Chatellus, Phys. Rev. Lett. **112**, 213902 (2014).
[12] J. A. Rice, *Mathematical Statistics and Data Analysis* (Duxbury Press, Berkeley, 1995).
[13] U. Hassan and M. S. Anwar, Eur. J. Phys. **31**, 453 (2010).
[14] M. Ricci, F. De Martini, N. J. Cerf, R. Filip, J. Fiurášek, and C. Macchiavello, Phys. Rev. Lett. **93**, 170501 (2004).
[15] U. L. Andersen, R. Filip, J. Fiurášek, V. Josse, and G. Leuchs, Phys. Rev. A **72**, 060301 (2005).
[16] M. Lassen, L. S. Madsen, M. Sabuncu, R. Filip, and U. L. Andersen, Phys. Rev. A **82**, 021801 (2010).
[17] C. Ferrie, New J. Phys. **16**, 093035 (2014).
[18] R. Maram, J. Van Howe, M. Li, and J. Azaña, Nat. Commun. **5**, 5163 (2014).
[19] M. V. Berry and S. Klein, J. Mod. Opt. **43**, 2139 (1996).
[20] H. C. Rosu, J. P. Treviño, and H. Cabrera, Int. J. Mod. Phys. B **20**, 1860 (2006).
[21] A. Malacarne and J. Azaña, Opt. Express **21**, 4139 (2013).
[22] R. Maram and J. Azaña, Opt. Express **21**, 28824 (2013).
[23] J. Caraquitena, M. Beltrán, R. Llorente, J. Martí, and M. Muriel, Opt. Lett. **36**, 858 (2011).
[24] A. Yariv, *Optical Electronics* (Oxford University Press, Oxford, 1995).
[25] B. Everitt, *The Cambridge Dictionary of Statistics* (Cambridge University Press, Cambridge, 1998).